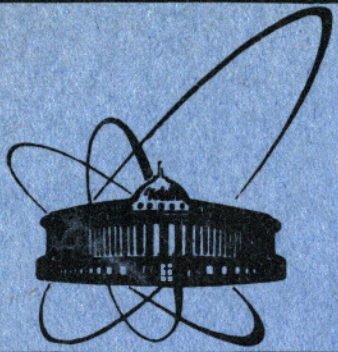

объединенный
институт
ядерных
исследований
дубна

E1-84-164

M.Bubak, V.M.Bystritsky, A.Guła

KINETIC FORMULAE FOR $(D+D)_\mu$ AND $(T+T)_\mu$ MUON-CATALYZED NUCLEAR SYNTHESIS

Submitted to "Nuclear Fusion"

1984

1. INTRODUCTION

The advent of the exciting results from Los Alamos [1] which indicate that neutron yield from the muon-catalyzed nuclear synthesis $(D+T)\mu \rightarrow (^4He + n)\mu$ may be even higher than previously expected [2-4] lays open the possibility of viewing the muon-catalysis as a potential source of nuclear energy [5]. The μ-atomic and μ-molecular processes leading to nuclear fusion in the $dt\mu$ molecule deserve now a closer look. However, in experiments with the D_2-T_2 targets, the presence of competing channels leading to fusion in the $dd\mu$ and $tt\mu$ molecules makes a more detailed investigation prohibitively complicated. The parameters characterizing these channels can be determined separately using pure deuterium and tritium targets. Such experiments are needed first to provide necessary input information for the analysis of the $(D+T)\mu$-fusion scheme.

The $(D+D)\mu$-fusion has already been studied in several experiments [6-8]. More data would be desirable, however, to allow better understanding of the processes involved and to resolve the discrepancies between the results of Refs. [7] and [8]. On the other hand, no data exist so far concerning the $(T+T)\mu$-fusion. These should be available soon from the experiment planned in Dubna [9].

The chain of processes leading to the muon-catalyzed fusion in a target consisting of one hydrogen isotope and possible admixtures of elements with $Z>1$ is depicted in Fig.1. The muon creates an excited μ-atom [10] which cascades down to the ground state in several intermediate steps. A μ-molecule is then formed, which possibly also undergoes deexcitation through one or more energy levels before fusion in it takes place. The fusion event ends one catalysis cycle. The muon which can be released in this process with probability $(1-\omega)$ reenters the chain to initiate the next cycle. At any node of the chain the muon may decay and, additionally, it can be irreversibly transferred to the element with $Z>1$, as indicated in the figure.

The transition rates between the nodes, λ_i, and the sticking coefficient, ω, which characterize the muon-catalysis chain can be most naturally determined from the time distribution of the fusion events ending the consecutive cycles and analogous distributions of the signatures of other processes in the chain. Such distributions are described by a set of particle-balance equations, one for each node in the sequence,

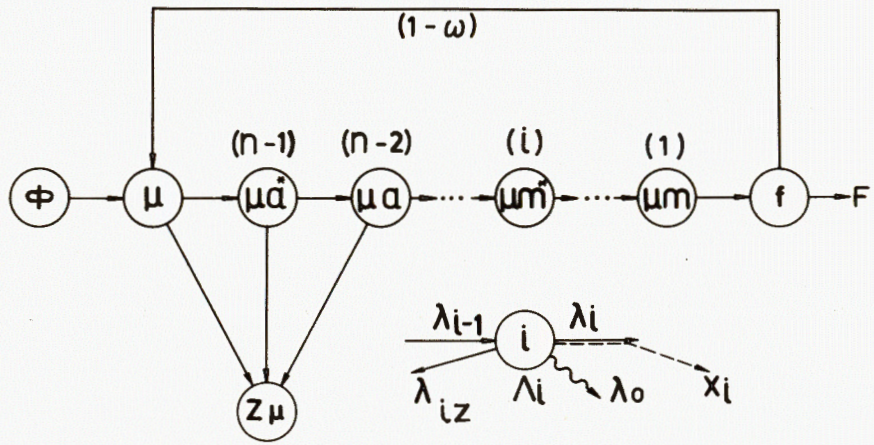

Fig.1. Schematic graph presenting the muon-catalysis fusion chain in a target consisting of one hydrogen isotope (D_2 or T_2) and possible admixtures of elements with $Z>1$.

which are usually referred to as kinetic equations. Solutions of the kinetic equations have been discussed in different approximations by several authors, both for the mixtures of hydrogen isotopes [11-16] and, in more detail, for the one-component targets [17-20]. So far, attention has been focused mainly on the "all-cycles" (AC) solutions which describe sums of the considered quantities taken over all cycles initiated by a single muon. Recently, the formulae have been also obtained which describe the separate cycles of the muon-catalysis chain in the one-component targets* [18-20]. Such a cycle-by-cycle description is better suited for experiments in which only a limited number of cycles is registered. In [18] it has been assumed that kinetics of the chain is solely determined by the process of μ-molecule formation. This is justified for the $(D+D)\mu$-fusion where the rates of other processes are expected to be much higher ($\gtrsim 10^9 s^{-1}$) [21] so that, at least for $t \gtrsim 10$ ns, their influence can be neglected. In [19,20] nuclear synthesis in the μ-molecule has been additionally taken into account to obtain the formulae relevant for the description of the $(T+T)\mu$ chain, where the corresponding fusion rate can be as low as $10^7 s^{-1}$ [22].

In the present paper we derive cycle-by-cycle formulae which enable one to introduce any number of intermediate steps

* In [20] an approximate cycle-by-cycle formula for the $(D+T)\mu$-fusion is also presented.

leading to the muon-catalysed synthesis, i.e., besides the processes mentioned above, the creation of μ-atoms and μ-molecules in the excited states and their deexcitation towards the ground state. Although the rates of these processes are expected to be rather high, we derive our formulae without any approximations and leave open the question of the magnitude of the transition rates.

By introducing appropriate admixtures of elements with $Z > 1$ information about the rates of processes in pure D_2 or T_2 can be supplemented to include the rates of muon transitions from hydrogen to heavier nuclei. Transitions to helium are here of particular interest as both ^3He and ^4He are produced in the $D_2 - T_2$ target and are probably the primary fuel poisoning factors to be taken into account.

2. FIRST CYCLE EQUATIONS

The kinetic equations describing the first cycle (no muon feedback) are:

$$\begin{aligned}
&\frac{dN_f(t)}{dt} = \Lambda_1 N_1(t) \\
&\frac{dN_1(t)}{dt} = -\lambda_1 N_1(t) + \lambda_2 N_2(t) \\
&\cdots\cdots\cdots\cdots\cdots\cdots\cdots\cdots \\
&\frac{dN_i(t)}{dt} = -\Lambda_i N_i(t) + \lambda_{i+1} N_{i+1}(t) \\
&\cdots\cdots\cdots\cdots\cdots\cdots\cdots\cdots \\
&\frac{dN_n(t)}{dt} = -\Lambda_n N_n(t) + \frac{d\phi(t)}{dt},
\end{aligned} \tag{1}$$

where $N_i(t)$ are particle numbers in each of the nodes in Fig.1, $\phi(t)$ represents the muon source, and

$$\Lambda_i = \lambda_i + \lambda_0 + \sum_z \lambda_{i,z} \,. \tag{2}$$

In Eq.(2) λ_i are transition rates between the nodes, $\lambda_0 = 0.455\ \mu s^{-1}$ is the muon decay rate and $\lambda_{i,z}$ are the corresponding rates of transitions $(i) \to (Z\mu)$. Let us choose also $N_i(t) = 0$, $\phi(t) = 0$ for $t < 0$.

The time distributions of signatures which can be associated with $(i) \to (i-1)$ transitions are given by:

$$x_i(t) = -\frac{dX_i(t)}{dt} = \lambda_i N_i(t) \,. \tag{3}$$

In particular, for the signatures of the fusion events we have:

$$F(t) = \frac{dN_f(t)}{dt} = \lambda_1 N_1(t) \tag{4}$$

and correspondingly for the time distribution of $Z\mu$-atoms

$$\frac{dN_{z\mu}}{dt} = \Sigma \lambda_{i,z} N_i(t) \,, \tag{5}$$

where summation goes over the muonic and μ-atomic nodes.

After taking the Laplace transform of Eq.(1) one obtaines immediately:

$$N_f(s) = G_1^{(n)}(s) \cdot \phi(s) \,, \tag{6}$$

where

$$G_1^{(n)}(s) = \prod_{i=1}^{n} \frac{\lambda_i}{s + \Lambda_i} \,, \tag{7}$$

s denotes the Laplace transform parameter and n is the number of nodes in the chain.

3. "ALL-CYCLES" (AC) SOLUTION

The solution for all cycles is readily obtained from Eqs. (6-7) by closing the muon feedback loop:

$$N_f^{(AC)}(s) = G^{(n)}(s) \cdot \phi(s) \,, \tag{8}$$

where

$$G^{(n)}(s) = \frac{G_1^{(n)}(s)}{1 - (1-\omega) \cdot G_1^{(n)}(s)} \,. \tag{9}$$

For $\phi(t)$ given by the step function which corresponds to one muon entering the target at $t = 0$, the Laplace transform of the (AC)-time distribution of fusion events is:

$$F^{(AC)}(s) = G^{(n)}(s) = \frac{\prod_{i=1}^{n} \lambda_i}{\prod_{i=1}^{n} (s + \Lambda_i) - (1-\omega) \cdot \prod_{i=1}^{n} \lambda_i} \,. \tag{10}$$

The most immediate result following from Eq.(10) is the formula for the (AC)-yield of fusion events:

$$Y^{(AC)} = \int_0^\infty F^{(AC)}(t)\, dt = F^{(AC)}(s=0) = \frac{\prod_{i=1}^{n} \lambda_i}{\prod_{i=1}^{n} \Lambda_i - (1-\omega) \cdot \prod_{i=1}^{n} \lambda_i} \,. \tag{11}$$

The (AC)-time distribution of fusion events can be obtained by taking the inverse transform of (10):

$$F^{(AC)}(t) = \left(\prod_{i=1}^{n} \lambda_i\right) \cdot \sum_{i=1}^{n} \frac{e^{r_i t}}{\prod_{\substack{j=1 \\ j\neq i}}^{n} (r_i - r_j)}, \qquad (12)$$

where r_i are zeros of the denominator in the RHS of Eq.(10). Since $(1-\omega) < 1$ and $\Lambda_i > \lambda_i$ all r_i are negative.

4. CYCLE-BY-CYCLE KINETICS

The time distributions for the separate cycles are of great importance both for understanding the kinetics of the muon-catalyzed fusion and for the analysis of the experimental data.

Let us expand $F^{(AC)}(s)$ in terms of $(1-\omega)$. From Eq.(9) one has

$$F^{(AC)}(s) = \sum_{k=1}^{\infty} (1-\omega)^{k-1} \cdot [G_1^{(n)}(s)]^k = \sum_{k=1}^{\infty} F_k(s). \qquad (13)$$

In time variable Eq.(13) reads:

$$F_k(t) = (1-\omega)^{k-1} \cdot \underbrace{F_1(t) * F_1(t) * \ldots * F_1(t)}_{k\text{-fold convolution}} \qquad (14)$$

which, in an obvious interpretation[19], gives us the time distribution of fusion events ending the k-th cycle.

In analogy to Eq.(11), the k-th cycle yield is then

$$Y_k = (1-\omega)^{k-1} \cdot \left(\prod_{i=1}^{n} \frac{\lambda_i}{\Lambda_i}\right)^k. \qquad (15)$$

Again, the k-th cycle time distribution of fusion events can be written as:

$$F_k(t) = (1-\omega)^{k-1} \cdot \left(\prod_{i=1}^{n} \lambda_i\right)^k \cdot Q_k^{(n)}(\Lambda_1, \ldots, \Lambda_n, t), \qquad (16)$$

where

$$Q_k^{(n)}(\Lambda_1, \ldots, \Lambda_n, t) = \mathcal{L}^{-1}\left[\left(\prod_{i=1}^{n} \frac{1}{s+\Lambda_i}\right)^k\right]. \qquad (17)$$

The explicit form of the inverse Laplace transform in Eq.(17) is:

$$Q_k^{(n)}(\Lambda_1, \ldots, \Lambda_n, t) = \frac{(-1)^{(n-1)k}}{[(k-1)!]^{n-1}} \sum_{j=1}^{k} \frac{t^{k-j}}{(j-1)!\,(k-j)!} \times \qquad (18)$$

$$\times \sum_{i=1}^{n} e^{-\Lambda_i \cdot t} \cdot \sum_{\substack{\ell_1, \ldots, \ell_p, \ldots \ell_n \\ p\neq i}} \binom{j-1}{\ell_1, \ldots \ell_p, \ldots \ell_n} \frac{(k-1+\ell_1)! \ldots (k-1+\ell_n)!}{\prod_{\substack{p=1 \\ p\neq i}}^{n} (\Lambda_i - \Lambda_p)^{k+\ell_p}}.$$

In the Appendix we list the formulae for the first four nodes which can be useful in the analysis of the experimental data from the $D_2(T_2)$ targets.

The yields and time distributions of signatures associated with $(i) \to (i-1)$ transitions in the k-th cycle of the μ-catalysis chain can be found from the relation:

$$x_i(s) = (1-\omega)^{k-2} \cdot [G_1^{(n)}(s)]^{k-1} \cdot (1-\omega) \cdot \prod_{j=n}^{i} \frac{\lambda_j}{s+\Lambda_j}, \qquad (19)$$

which represents the convolution of $F_{k-1}(t)$ for the preceding $(k-1)$ cycles with the function describing the k-th cycle, truncated at the i-th node.

If there are more than one nuclear synthesis channels (as in the D + D fusion) the time distribution of their signatures can be obtained by substituting in Eqs.(15-19):

$$(1-\omega)\lambda_1 \to \sum_j (1-\omega_j)\lambda_{1,j} \qquad (20)$$

with

$$\lambda_1 = \sum_j \lambda_{1,j} \qquad (21)$$

and multiplying the resulting expression by the branching ratio $b_j = \lambda_{1,j}/\lambda_1$, $\lambda_{1,j}$ being the transition rate into the j-th channel and ω_j the corresponding sticking coefficient.

In most experiments the signatures of fusion and other internode transitions are detected with efficiency $\epsilon < 1$. According to the arguments of Ref.[18] the Laplace transform of the time distribution of the first registered cycle is:

$$\overline{F_1}(s) = \epsilon \cdot \sum_{k=1}^{\infty} (1-\epsilon)^{k-1} \cdot F_k(s) \qquad (22)$$

which, using Eqs. (10,13), can be written as:

$$\overline{F_1}(s) = \epsilon \cdot \frac{\prod_{i=1}^{n} \lambda_i}{\prod_{i=1}^{n} (s+\Lambda_i) - (1-\omega)\cdot(1-\epsilon)\cdot \prod_{i=1}^{n} \lambda_i}, \qquad (23)$$

where ϵ is the experimental registration efficiency of fusion events. Analogously to Eq.(14) the corresponding expression for the k-th registered cycle is

$$\overline{F_k}(s) = (1-\omega)^{k-1} \cdot [\overline{F}_1(s)]^k . \qquad (24)$$

Thus $\overline{F_k}(t)$ can be obtained by substituting in Eq.(16)

$$(\Pi\lambda_i) \to \epsilon\Pi\lambda_i , \quad \Lambda_i \to -s_i , \qquad (25)$$

where s_i are zeros of the denominator in Eq.(23). Analogously, for several fusion channels, substitutions (20,21) should be made and ϵ replaced in (23) by $\epsilon_j b_j$, where ϵ_j is the registration efficiency for the j-th channel, and b_j the corresponding branching ratio.

5. DISCUSSION

To illustrate the obtained dependences we show in Figs.2-5 the time distributions of fusion events ending the first few cycles*. In all figures $\omega = 0.1$ which is approximately the value of the sticking coefficient in both $(D+D)\mu \to (^3He + n)\mu$ and $(T+T)\mu \to (^4He + n)\mu$.

Fig.2 illustrates, for a one-component target (concentration of admixtures $C_z = 0$), introducing of the consecutive nodes differing by one order of magnitude: $\lambda_1 = 1\mu s^{-1}$ (1 node); $\lambda_1, \lambda_2 = 10\mu s^{-1}$ (2 nodes); $\lambda_1, \lambda_2, \lambda_3 = 100\ \mu s^{-1}$ and $\lambda_1, \lambda_2, \lambda_3, \lambda_4 = 1000\ \mu s^{-1}$. It is seen that switching on an additional node with λ by one order of magnitude larger than the previous one gives in this range of λ_i a significant effect even at quite large t, especially in higher cycles. This effect is even more pronounced for $\epsilon < 1$ which is rather obvious, as many cycles contribute there to the first registered cycle. The apparent advantage of observing the contributions from high $-\lambda$ nodes at large t in experiments with small ϵ is, however, reduced by the decrease in statistics. In planning the experiment attention should be given to the interplay of these two factors.

In Fig.3 we illustrate the situation which may arise in the experiments with pure ($C_z = 0$) liquid deuterium and tritium targets. The curves in Fig.3a are for (D+D)μ-fusion where $\lambda_1 = \lambda_m \approx 0.1\ \mu s^{-1}$ ($dd\mu$-formation), $\lambda_2 = \lambda_f \approx 10^3\ \mu s^{-1}$ (fusion in $tt\mu$)[23] and $\lambda_3 = \lambda_{casc} \approx 5\times10^4 s^{-1}$ (cascade to the ground state

*The curves were obtained using the four-node formula (A.4) of the Appendix. Curves for fewer nodes (n = 1÷3) were computed using also Eq.(A.4) and switching-off some of the nodes by putting the corresponding λ_i very large.

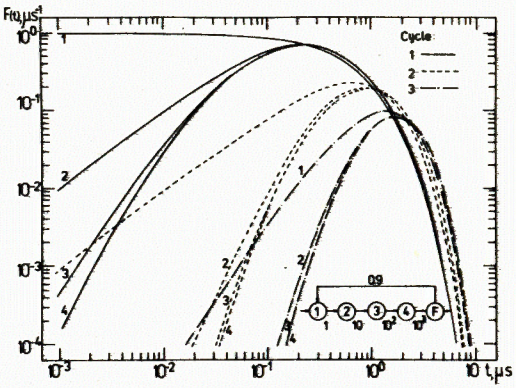

Fig.2. Time distributions of the first three cycles initiated by a single muon at t = 0 for $\lambda_1 = 1\ \mu s^{-1}$ $\lambda_2 = 10\ \mu s^{-1}$, $\lambda_3 = 100\ \mu s^{-1}$ and $\lambda_4 = 1000\mu s^{-1}$. The number of nodes included in an increasing order is indicated at the curves. Registration efficiency is $\epsilon = 1$ and no contaminations by Z>1 are present.

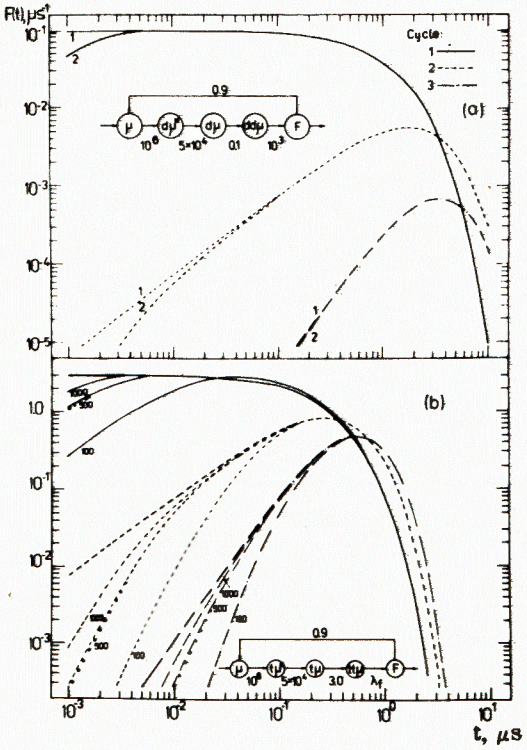

Fig.3. Time distributions of the first three cycles initiated by a single muon at t = 0: a) for $\lambda_m = 0.1\ \mu s^{-1}$, $\lambda_f = 10^3\ \mu s^{-1}$ $\lambda_{casc} = 5\cdot10^4\mu s^{-1}$, $\lambda_a = 10^6\ \mu s^{-1}$ (as in the case of (D+D)μ-fusion). Contributions from λ_{casc} and λ_a become visible only below 1 ns. b) for $\lambda_m = 3\ \mu s^{-1}$, $\lambda_{casc} = 5\cdot10^4\mu s^{-1}$ $\lambda_a = 10^6\mu s^{-1}$ and varying λ_f ((T+T)μ-fusion). The values of λ_f are indicated at the curves. Thick lines are for 1-node solution (λ_m only), and the thin ones for 2-nodes (λ_f included). For $\lambda_f = 500\ \mu s^{-1}$ the effect of including λ_{casc} is indicated by the dots. Other comments as in Fig.2.

in $d\mu$) [24]. According to the theoretical predictions, the fusion rate in the $tt\mu$ molecule, λ_f, may have values between $10^1 \div 10^3\ \mu s^{-1}$ [22], and $\lambda_1 = \lambda_m \approx 3\ \mu s^{-1}$ [25]. Fig.3b shows how inclusion of different λ_f modifies the 1-node (λ_1 only) distribution of the first two cycles. It is seen that in the second cycle $\lambda_2 = \lambda_f = 100\ \mu s^{-1}$ gives a significant contribution even at $t \approx 100$ ns. The effect of λ_3 becomes visible in the region of a few nanoseconds.

Figs.4-5 present the effect of contaminating the liquid tritium target by adding admixtures of heavier elements. In Fig.4 the situation is shown in which only $\Lambda_2 = \lambda_m + \lambda_0 + \Sigma\lambda_{\mu,z}$ is significantly modified. Λ_1, which is determined by the fusion rate, λ_f, is not affected by the admixtures. As is expected, the large time tails become steeper and differ considerably for different hypotheses. The curves are determined practically by the first two nodes, the effect of λ_3 becoming pronounced only below 10 ns.

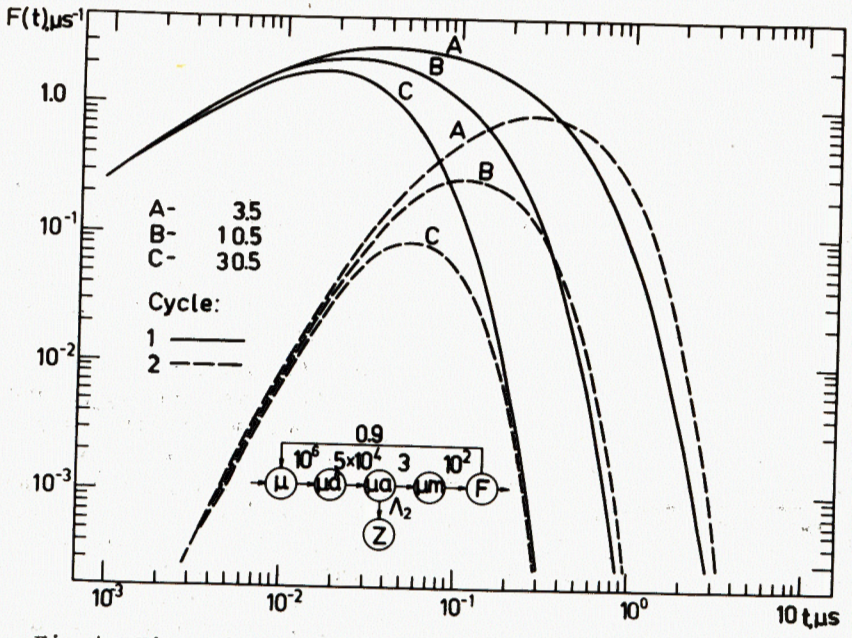

Fig.4. Time distributions of the first two cycles for $\epsilon = 1$, $\lambda_m = 3\ \mu s^{-1}$, $\lambda_f = 100\ \mu s^{-1}$, $\lambda_{casc} = 5 \cdot 10^4\ \mu s^{-1}$, $\lambda_a = 10^6\ \mu s^{-1}$, Λ_2 is varied as indicated in the figure, $\Lambda_i = \lambda_i + \lambda_0$ for $i \neq 2$.

Analogous curves, in which Λ_2 is fixed and different hypotheses for Λ_3 are tried, are shown in Fig.5a and similarly

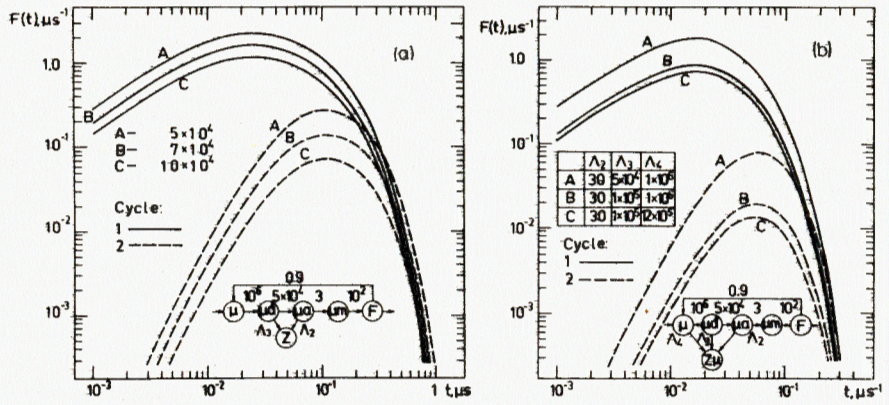

Fig.5. Time distributions of the first and second cycle for $\epsilon = 1$, $\lambda_f = 100\ \mu s^{-1}$, $\lambda_m = 3\ \mu s^{-1}$, $\lambda_{casc} = 5 \cdot 10^4\ \mu s^{-1}$, $\lambda_a = 10^6 \mu s^{-1}$. a) Λ_2 is fixed at $10.5\ \mu s^{-1}$ and Λ_3 is varied as indicated in the figure, b) Λ_2 is fixed ($30\ \mu s^{-1}$), Λ_3 and Λ_4 are varied as indicated in the figure.

for Λ_2, Λ_3 fixed and Λ_4 varying, in Fig.5b. Presence of higher nodes is strongly reflected in the time distributions. However, in the region of $t \gtrsim 10$ ns the effect is practically reduced to multiplication of the curve for $C_z = 0$ by a factor λ_i/Λ_i which is obvious from Eqs. (16-18). More delicate effects appear only below 1 ns. Let us remark that the modification of Λ_i is determined by the product of the known heavy element concentration, C_z, and the unknown exchange rate, $\lambda_{i,z}$.

6. CONCLUSIONS

The formulae presented above provide a practical tool for the interpretation of the experimental data on the muon-catalysed fusion in a D_2 or T_2 target. Let us first remark that the time distributions (16-18) are invariant with respect to permutation of λ_i and independently of Λ_i, which is a generalization of the result of Ref. [17,19]. Thus, ascribing the experimental values to the particular nodes will require the use of variation of λ_i and Λ_i with temperature (λ_m), target density* (λ_m, λ_a) or heavy element concentration (Λ_a, Λ_{casc}, Λ_m). In this respect measuring the signatures

* This effect was discussed in detail for the 2-node AC-solution in Ref. [17].

of other transitions in the chain would provide useful additional information.

As is seen from the discussion in the previous Section, even relatively high transition rates can be appreciated in the 10-100 ns region, especially in high statistics measurements of the time distributions of the second or third cycle. Information from such experiments supplemented with the data obtained in other approaches will constitute a helpful input for the analysis of (D+T)μ-fusion chain.

ACKNOWLEDGEMENTS

The authors are indebted to Prof. L.I.Ponomarev for the stimulating discussions which have led to this investigation. They also thank their colleagues M.P.Faifman, V.S.Melezhik, L.I.Menshikov and J.Woźniak for helpful conversations. Two of the authors (M.B. and A.G.) thank Prof. V.P.Dzhelepov for his hospitality during their stay at JINR on leave from AGH, Cracow, Poland. One of them (M.B.) expresses his gratitude to Dr. E.P.Shabalin for creating conditions which enabled him to participate in this work.

APPENDIX

The explicit expressions for $Q_k^{(n)}(\Lambda_1,\ldots,\Lambda_n,t)$ according to Eq.(18) are:

$$Q_k^{(1)}(\Lambda_1,t) = \frac{t^{k-1}}{(k-1)!}\cdot e^{-\Lambda_1\cdot t}, \qquad (A.1)$$

$$Q_k^{(2)}(\Lambda_1,\Lambda_2,t) = \frac{(-1)^k}{(k-1)!}\cdot\sum_{j=1}^{k}\frac{(k+j-2)!}{(j-1)!(k-j)!}\cdot t^{k-j}\times$$

$$\times\left[\frac{e^{-\Lambda_1\cdot t}}{(\Lambda_1-\Lambda_2)^{k+j-1}}+\frac{e^{-\Lambda_2\cdot t}}{(\Lambda_2-\Lambda_1)^{k+j-1}}\right], \qquad (A.2)$$

$$Q_k^{(3)}(\Lambda_1,\Lambda_2,\Lambda_3,t) = \frac{1}{[(k-1)!]^2}\cdot\sum_{j=1}^{k}\frac{t^{k-j}}{(k-j)!}\cdot\sum_{\ell=0}^{j-1}\frac{(k+j-2-\ell)!(k-1+\ell)!}{\ell!(j-1-\ell)!}\times$$

$$\times\left[\frac{e^{-\Lambda_1\cdot t}}{(\Lambda_1-\Lambda_2)^{k+j-1-\ell}(\Lambda_1-\Lambda_3)^{k+\ell}}+\frac{e^{-\Lambda_2\cdot t}}{(\Lambda_2-\Lambda_1)^{k+j-1-\ell}(\Lambda_2-\Lambda_3)^{k+\ell}}+\right.$$

$$\left.+\frac{e^{-\Lambda_3\cdot t}}{(\Lambda_3-\Lambda_1)^{k+j-1-\ell}(\Lambda_3-\Lambda_2)^{k+\ell}}\right], \qquad (A.3)$$

$$Q_k^{(4)}(\Lambda_1,\Lambda_2,\Lambda_3,\Lambda_4,t) = \frac{(-1)^k}{[(k-1)!]^3}\cdot\sum_{j=1}^{k}\frac{t^{k-j}}{(k-j)!}\times$$

$$\times\sum_{\ell=0}^{j-1}\sum_{m=0}^{j-1-\ell}\frac{(k-2+j-\ell-m)!(k-1+m)!(k-1+\ell)!}{\ell!m!(j-1-\ell-m)!}\times$$

$$\times\left[\frac{e^{-\Lambda_1\cdot t}}{(\Lambda_1-\Lambda_2)^{k+j-1-\ell-m}(\Lambda_1-\Lambda_3)^{k+m}\cdot(\Lambda_1-\Lambda_4)^{k+\ell}}+\right.$$

$$+\frac{e^{-\Lambda_2\cdot t}}{(\Lambda_2-\Lambda_1)^{k+j-1-\ell-m}(\Lambda_2-\Lambda_3)^{k+m}\cdot(\Lambda_2-\Lambda_4)^{k+\ell}}+$$

$$+\frac{e^{-\Lambda_3\cdot t}}{(\Lambda_3-\Lambda_1)^{k+j-1-\ell-m}\cdot(\Lambda_3-\Lambda_2)^{k+m}\cdot(\Lambda_3-\Lambda_4)^{k+\ell}}+$$

$$\left.+\frac{e^{-\Lambda_4\cdot t}}{(\Lambda_4-\Lambda_1)^{k+j-1-\ell-m}(\Lambda_4-\Lambda_2)^{k+m}\cdot(\Lambda_4-\Lambda_3)^{k+\ell}}\right]. \qquad (A.4)$$

In particular, for n = 1 and 2 our formulae coincide with the one- and two-node approximations of Refs.[18] and [19], respectively.

For the time distributions of the registered cycles (registration efficiency $\epsilon < 1$) substitutions (25) have to be used. When several fusion channels are present the formulae should be modified as described in Section 4.

REFERENCES

1. Jones S.E. et al. Atomkernenergie/Kerntechnik, 1983, 43, p.179; Phys.Rev.Lett., 1983, 51, p.1757.
2. Gershtein S.S., Ponomarev L.I. Phys.Lett., 1977, 72B, p.80.
3. Vinitsky S.I. et al. Zh.Eksp.Teor.Fiz., 1978, 74, p.849 (English transl.Sov.Phys., JETP, 1979, 47, p.444).
4. Bystritsky V.M. et al. Phys.Lett., 1980, 94B, p.476; Zh.Eksp.Teor.Fiz., 1981, 80, p.1700 (English transl.Sov. Phys., JETP, 1981, 53, p.877).
5. Petrov Yu.V. Nature, 1980, 285, p.466.
6. Doede J.H. et al. Phys.Rev., 1963, 132, p.1782; Kammel P. et al. Phys.Lett., 1982, 112B, p.319.

7. Bystritsky V.M. et al. Zh.Eksp.Teor.Fiz., 1979, 76, p.460. (English transl.Sov.Phys., JETP, 1979, 49, p.232).
8. Balin D.V. et al. Preprint LINP, 895, Leningrad, 1983.
9. Bystritsky V.M. et al. JINR, P13-82-378, Dubna, 1982 (in Russian); JINR, P13-84-59, Dubna, 1984 (in Russian).
10. Gershtein S.S., Ponomarev L.I. In: Muon Physics (Eds. V.M.Hughes and C.S.Wu). Academic Press, New York, 1975, vol.III, p.141.
11. Gershtein S.S. et al. Zh.Eksp.Teor.Fiz., 1980, 78, p.2099. (English transl.Sov.Phys., JETP, 1980, 51, p.1053).
12. Somov L.N. JINR, P4-81-852, Dubna, 1981 (in Russian).
13. Takahashi H. et al. Atomkernenergie/Kerntechnik, 1980, 36, p.195.
14. Lie S.G., Harms A.A. Nucl.Sci.Eng., 1982, 80, p.124.
15. Sguigna A.P., Harms A.A. Atomkernenergie/Kerntechnik, 1983, 43, p.191.
16. Kumar A. Atomkernenergie/Kerntechnik, 1983, 43, p.203; Kammel P. et al. Atomkernenergie/Kerntechnik, 1983, 43, p.195.
17. Bystritsky V.M. et al. JINR, E1-83-690, Dubna, 1983.
18. Zinov V.G., Somov L.N., Filchenkov V.V. JINR, P15-82-478, Dubna, 1982.
19. Bystritsky V.M., Guła A., Woźniak J. JINR, E1-84-26, Dubna, 1984.
20. Zinov V.G., Somov L.N., Filchenkov V.V. JINR, P4-84-45, Dubna, 1984.
21. See, e.g.: Ponomarev L.I. Atomkernenergie/Kerntechnik, 1983, 43, p.175.
22. Melezhik V.S. JINR, P4-81-463, Dubna, 1981 (in Russian).
23. Bogdanova L.M. et al. Phys.Lett., 1982, 115B, p.171.
24. Markushin V.E. Zh.Eksp.Teor.Fiz., 1981, 80, p.35 (English transl.Sov. Phys., JETP, 1981, 53, p.17).
25. Ponomarev L.I., Faifman M.P. Zh.Eksp.Teor.Fiz., 1976, 71, p.1689 (English transl.Sov.Phys., JETP, 1976, 44, p.886).

Received by Publishing Department
on March 16,1984.

Бубак М., Быстрицкий В.М., Гула А. E1-84-164

Формулы кинетики мюонного катализа реакций ядерного синтеза $(D+D)_\mu$ и $(T+T)_\mu$

В работе приводятся основные формулы кинетики, полученные при рассмотрении произвольного числа μ-атомных и μ-молекулярных переходов, предшествующих мюонному катализу реакций ядерного синтеза в D_2 или T_2 мишени с возможными добавками примесей с $Z>1$. Обсуждается применение найденных формул для анализа экспериментальных данных.

Работа выполнена в Лаборатории ядерных проблем ОИЯИ.

Препринт Объединенного института ядерных исследований. Дубна 1984

Bubak M., Bystritsky V.M., Guła A. E1-84-164

Kinetic Formulae for $(D+D)_\mu$ and $(T+T)_\mu$ Muon-Catalyzed Nuclear Synthesis

General kinetic formulae taking into account an arbitrary number of μ-atomic and μ-molecular transitions in the chain leading to the muon-catalyzed nuclear synthesis in a D_2 or T_2 target with possible $Z>1$ contaminations are derived. Application of the obtained formulae to the analysis of the experimental data is discussed.

The investigation has been performed at the Laboratory of Nuclear Problems, JINR.

Preprint of the Joint Institute for Nuclear Research. Dubna 1984